

# CENTRAL SCHEMES FOR POROUS MEDIA FLOW

E. ABREU<sup>1</sup>, F. FURTADO<sup>2</sup>, F. PEREIRA<sup>1</sup> AND S. RIBEIRO<sup>1</sup>

<sup>1</sup> State University of Rio de Janeiro, Nova Friburgo, RJ 28630-050, Brazil.

<sup>2</sup> University of Wyoming, Laramie, WY 82071-3036, U.S.A.

## ABSTRACT

We are concerned with central differencing schemes for solving scalar hyperbolic conservation laws arising in the simulation of multiphase flows in heterogeneous porous media. We compare the Kurganov-Tadmor (KT) [Kurganov, et al., 2000] semi-discrete central scheme with the Nessyahu-Tadmor (NT) [Nessyahu, et al., 1990] central scheme. The KT scheme uses more precise information about the local speeds of propagation together with integration over nonuniform control volumes, which contain the Riemann fans. These methods can accurately resolve sharp fronts in the fluid saturations without introducing spurious oscillations or excessive numerical diffusion, although the numerical dissipation in the (KT) scheme is smaller than in the original NT scheme.

Numerical simulations are presented for two-phase, two-dimensional flow problems in heterogeneous formations. We find the KT scheme to be considerably less diffusive, particularly in the presence of viscous fingers, which lead to strong restrictions on the time step selection; however, the KT scheme may produce incorrect boundary behavior.

## 1. INTRODUCTION

We consider a model for two-phase flow, immiscible and incompressible displacement in heterogeneous porous media. The governing equations are highly nonlinear and leads to shock formation, and with or without diffusive terms they are of practical importance in petroleum engineering [D. W. Peaceman, 1977, Chavent, et al., 1986] (see also [Furtado, et al., 2003] and the references therein for recent studies for the scale-up problem for such equations).

The conventional theoretical description of two-phase (oil-water) flow in a porous medium, in the limit of vanishing capillary pressure, is via Darcy's law coupled to the Buckley-Leverett equation. The two phases will be referred to as water and oil, and indicated by the subscripts  $w$  and  $o$ , respectively. We also assume that the two fluid phases saturate the pores. With no sources or sinks, and neglecting the effects of gravity these equations are (see Peaceman [D. W. Peaceman, 1977]):

$$\nabla \cdot \mathbf{v} = 0, \quad \mathbf{v} = -\lambda(s)K(\mathbf{x})\nabla p, \quad (1)$$

$$\frac{\partial s}{\partial t} + \nabla \cdot (f(s)\mathbf{v}) = 0. \quad (2)$$

Here,  $\mathbf{v}$  is the total seepage velocity,  $s$  is the water saturation,  $K(\mathbf{x})$  is the absolute permeability, and  $p$  is the pressure. The constant porosity has been scaled out by a

change of the time variable. The constitutive functions  $\lambda(s)$  and  $f(s)$  represent the total mobility and the fractional flow of water, respectively.

We are concerned with numerical schemes for solving scalar hyperbolic conservation laws arising in the simulation of multiphase flows in multidimensional heterogeneous porous media. These schemes are non-oscillatory and enjoy the main advantage of Godunov-type central schemes: simplicity, i.e., they employ neither characteristic decomposition nor approximate Riemann solvers. This makes them universal methods that can be applied to a wide variety of physical problems, including hyperbolic systems of conservation laws.

We compare the Kurganov-Tadmor (KT) [Kurganov, et al., 2000] semi-discrete central scheme with the Nessyahu-Tadmor (NT) [Nessyahu, et al., 1990] central scheme for numerical simulations for two-phase, two-dimensional flow in heterogeneous formations. These methods can accurately resolve sharp fronts in the fluid saturations without introducing spurious oscillations or excessive numerical diffusion. The NT scheme has recently been used in the numerical investigation of non-classical waves in multidimensional three-phase (oil-gas-water) flows in petroleum reservoirs (see [Abreu, et al., 2004b, Abreu, et al., 2004a, Abreu, et al., 2004d, Abreu, et al., 2004c]).

We find the KT scheme to be considerably less diffusive, particularly in the presence of viscous fingers, which lead to strong restrictions on the time step selection. On the other hand the KT may produce incorrect boundary behavior in a typical geometry used in the study of porous media flows: the quarter of a five spot.

This paper is organized as follows. In Section 2 we discuss our strategy for solving numerically the model for two-phase flows, immiscible and incompressible displacement in heterogeneous porous media introduced in Section 1. In Section 3 we will discuss the application of the central differencing schemes for porous media flow. In Section 4 we present the computational solutions for the model problem considered here and our conclusions.

## 2. NUMERICAL APPROXIMATION OF TWO-PHASE FLOW

**2.1. Operator splitting for two-phase flow.** An operator splitting technique is employed for the computational solution of the saturation equation (2) and the pressure equation (1) in which are solved sequentially with distinct time steps. This method has proved to be computationally efficient in producing accurate numerical solutions for two-phase flow [Furtado, et al., 2003, Douglas, J., Jr., et al., 1997]. (see also [Abreu, et al., 2004b, Abreu, et al., 2004a, Abreu, et al., 2004d, Abreu, et al., 2004c] to the application of this strategy for three-phase flow problems.)

Typically, for computational efficiency, larger time steps are used for the pressure calculation (1). The splitting allows time steps for the pressure-velocity calculation that are longer than those for the convection calculation. Thus, we introduce two time steps:  $\Delta t_c$  for the solution of the hyperbolic problem for the convection, and  $\Delta t_p$  for the pressure-velocity calculation so that  $\Delta t_p \geq \Delta t_c$ . We remark that in practice, variable time steps are always useful, especially for the convection micro-steps subject dynamically to a *CFL* condition.

For the global pressure solution (the pertinent elliptic equation), we use a (locally conservative) hybridized mixed finite element discretization equivalent to cell-centered finite

differences [Furtado, et al., 2003, Douglas, J., Jr., et al., 1997], which effectively treats the rapidly changing permeabilities that arise from stochastic geology and produces accurate velocity fields. The oil pressure and the Darcy velocity are approximated at times  $t^m = m\Delta t_p$ ,  $m = 0, 1, 2, \dots$ . The linear algebra system resulting from the discretized equations can be solved by a preconditioned conjugate gradient procedure (PCG) or by a multi-grid procedure ([Douglas, J., Jr., et al., 1997]).

We use high resolution numerical central schemes (see [Nessyahu, et al., 1990] and [Kurganov, et al., 2000]) for solving the scalar hyperbolic conservation laws arising in the convection of the fluid phases in heterogeneous porous media for two-phase flows - we will discuss the application of these schemes for two-phase flows in the numerical section 4. These methods can accurately resolve sharp fronts in the fluid saturations without introducing spurious oscillations or excessive numerical diffusion.

The saturation equation is approximated at times  $t_\kappa^m = t^m + \kappa\Delta t_c$  for  $t^m < t_\kappa^m \leq t^{m+1}$  that take into account the advective transport of water.

We remark that we must specify the water saturation at  $t = 0$ .

A detailed description of the numerical method that we employ for the solution of Eqs. (1)-(2) can be found in [Furtado, et al., 2003] and references therein (see also [Abreu, et al., 2004a, Abreu, et al., 2004d] for applications of the operator splitting technique for three phase flows that takes into account capillary pressure (diffusive effects)).

### 3. CENTRAL DIFFERENCING SCHEMES FOR POROUS MEDIA FLOW

In this section, we shall discuss the application and performance of the family of high resolution, non-oscillatory, conservative central differencing scheme, introduced by Nessyahu and Tadmor (NT) [Nessyahu, et al., 1990] and Kurganov and Tadmor (KT), for numerical approximation of the scalar hyperbolic conservation law modeling the convective transport of the fluid phases in two-phase flows and its coupling with lowest order Raviart-Thomas [Raviart P-A., et al., 1977] locally conservative mixed finite elements for the associated elliptic (velocity-pressure part) problem [Abreu, et al., 2004a].

These schemes enjoy the main advantage of Godunov-type central schemes: simplicity, i.e., they employ neither characteristic decomposition nor approximate Riemann solvers. This makes them universal methods that can be applied to a wide variety of physical problems, including hyperbolic systems. In the following sections 3.1 and 3.2 we shall discuss the main ideas of the NT and KT central schemes coupled with the hybridized mixed finite element discretization mentioned above.

**3.1. The Nessyahu-Tadmor central scheme for two-phase flows.** Consider the following scalar hyperbolic conservation law,

$$\frac{\partial s}{\partial t} + \frac{\partial}{\partial x}(x_v f(s)) + \frac{\partial}{\partial y}(y_v f(s)) = 0, \quad (3)$$

where  $x_v \equiv x_v(x, y, t)$  and  $y_v \equiv y_v(x, y, t)$  denote the  $x$  and  $y$  components of the velocity field  $\mathbf{v}$  (see Eq. 1). Consider the cell averages,

$$s_{j,k}(t) \equiv \frac{1}{\Delta X \Delta Y} \int_{x_{j-\frac{1}{2}}}^{x_{j+\frac{1}{2}}} \int_{y_{k-\frac{1}{2}}}^{y_{k+\frac{1}{2}}} s(x, y, t) dx dy. \quad (4)$$

To approximate a solution to (3), at each time level  $t_\kappa^m$  for  $t^m < t_\kappa^m \leq t^{m+1}$ , we start with a piecewise bilinear approximation of the cell averages (4), defined by

$$P_{j,k}(x, y, t_\kappa^m) = s_{j,k}(t_\kappa^m) + (x - x_j) \frac{1}{\Delta X} (s_x)_{j,k}(t_\kappa^m) + (y - y_k) \frac{1}{\Delta Y} (s_y)_{j,k}(t_\kappa^m), \quad (5)$$

$$x_{j-\frac{1}{2}} \leq x \leq x_{j+\frac{1}{2}}, \quad y_{k-\frac{1}{2}} \leq y \leq y_{k+\frac{1}{2}}.$$

In Eq. (5),

$$(s_x)_{j,k}(t_\kappa^m) = \Delta X \cdot \frac{\partial}{\partial x} s(x_j, y_k, t_\kappa^m) + O(\Delta X)^2, \quad (s_y)_{j,k}(t_\kappa^m) = \Delta Y \cdot \frac{\partial}{\partial y} s(x_j, y_k, t_\kappa^m) + O(\Delta Y)^2, \quad (6)$$

denote the discrete slopes in the  $x$  and  $y$  directions, respectively.

The reconstruction (4)-(5) retains conservation, i.e.:

$$\frac{1}{\Delta X \Delta Y} \int_{x_{j-\frac{1}{2}}}^{x_{j+\frac{1}{2}}} \int_{y_{k-\frac{1}{2}}}^{y_{k+\frac{1}{2}}} P(x, y, t) dx dy = s_{j,k}(t). \quad (7)$$

The time evolution of this reconstruction is based on the integration of the conservation law (3) over staggered volumes  $I_{j+\frac{1}{2}, k+\frac{1}{2}} \times [t_\kappa^m, t_\kappa^m + \Delta t_c]$  (dashed grid in Figure 1). The piecewise bilinear approximation of the cell averages is evolved in time, and then the result is projected on the staggered cells (dashed grid)  $I_{j+\frac{1}{2}, k+\frac{1}{2}}$  to yield new cell averages (see Figure 1).

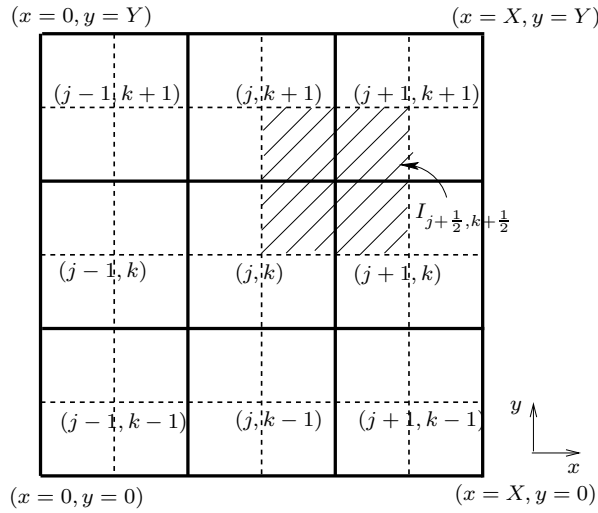


FIGURE 1. Evolution step at each time level  $t_\kappa^m$ ,  $t^m < t_\kappa^m \leq t^{m+1}$ , for the two-dimensional NT central differencing scheme.

The solution in the staggered grid obtained by the time evolution can be expressed as:

$$s_{j+\frac{1}{2}, k+\frac{1}{2}}(t_\kappa^m + \Delta t_c) = \bar{s}(x, y, t_\kappa^m + \Delta t_c) \equiv$$

$$\equiv \frac{1}{\Delta X \Delta Y} \int_{x_j}^{x_{j+1}} \int_{y_k}^{y_{k+1}} s(x, y, t_\kappa^m + \Delta t_c) dx dy, \quad x_j \leq x \leq x_{j+1}, \quad y_k \leq y \leq y_{k+1}. \quad (8)$$

By the conservation law (3) and following the same manipulations in [Nessyahu, et al., 1990] we get then the resulting new approximate cell averages ( $\alpha_x \equiv \frac{\Delta t_c}{\Delta X}$  and  $\alpha_y \equiv \frac{\Delta t_c}{\Delta Y}$ ):

$$\begin{aligned}
s_{j+\frac{1}{2},k+\frac{1}{2}}(t_\kappa^m + \Delta t_c) &= \frac{1}{4}(s_{j,k}(t_\kappa^m) + s_{j,k+1}(t_\kappa^m) + s_{j+1,k}(t_\kappa^m) + s_{j+1,k+1}(t_\kappa^m)) \\
&+ \frac{1}{16} \left[ (s_x)_{j,k}(t_\kappa^m) + (s_x)_{j,k+1}(t_\kappa^m) - (s_x)_{j+1,k}(t_\kappa^m) - (s_x)_{j+1,k+1}(t_\kappa^m) \right. \\
&\quad \left. + (s_y)_{j,k}(t_\kappa^m) - (s_y)_{j,k+1}(t_\kappa^m) + (s_y)_{j+1,k}(t_\kappa^m) - (s_y)_{j+1,k+1}(t_\kappa^m) \right] \quad (9) \\
&+ \frac{\alpha_x}{2} \left[ x_{v_{j,k}}(t_\kappa^m + \frac{\Delta t_c}{2}) f(s_{j,k}(t_\kappa^m + \frac{\Delta t_c}{2})) + x_{v_{j,k+1}}(t_\kappa^m + \frac{\Delta t_c}{2}) f(s_{j,k+1}(t_\kappa^m + \frac{\Delta t_c}{2})) \right. \\
&\quad \left. - x_{v_{j+1,k}}(t_\kappa^m + \frac{\Delta t_c}{2}) f(s_{j+1,k}(t_\kappa^m + \frac{\Delta t_c}{2})) - x_{v_{j+1,k+1}}(t_\kappa^m + \frac{\Delta t_c}{2}) f(s_{j+1,k+1}(t_\kappa^m + \frac{\Delta t_c}{2})) \right] \\
&+ \frac{\alpha_y}{2} \left[ y_{v_{j,k}}(t_\kappa^m + \frac{\Delta t_c}{2}) f(s_{j,k}(t_\kappa^m + \frac{\Delta t_c}{2})) + y_{v_{j+1,k}}(t_\kappa^m + \frac{\Delta t_c}{2}) f(s_{j+1,k}(t_\kappa^m + \frac{\Delta t_c}{2})) \right. \\
&\quad \left. - y_{v_{j,k+1}}(t_\kappa^m + \frac{\Delta t_c}{2}) f(s_{j,k+1}(t_\kappa^m + \frac{\Delta t_c}{2})) - y_{v_{j+1,k+1}}(t_\kappa^m + \frac{\Delta t_c}{2}) f(s_{j+1,k+1}(t_\kappa^m + \frac{\Delta t_c}{2})) \right].
\end{aligned}$$

The fluxes in (9) are smooth at the vertices of the cell defining the integration volume, since these vertices are located at the centers of non-staggered cells (see Figure 1). The spatial integrals in both the  $x$  and  $y$  directions are approximated by the second-order trapezoid quadrature rule and the temporal integrals are approximated by the midpoint quadrature rule under the restriction of a CFL-type constrain. As in the [Nessyahu, et al., 1990] procedure, the approximation of the fluxes in (9) make use of the midpoint values in time as a predictor step. So, by Taylor expansion and the conservation law (3) we can use

$$s_{j,k}(t_\kappa^m + \frac{\Delta t_c}{2}) = s_{j,k}(t_\kappa^m) - \frac{1}{2} \left[ x_{v_{j,k}}(t_\kappa^m) \frac{1}{\Delta X} (f_x)_{j,k}(t_\kappa^m) + y_{v_{j,k}}(t_\kappa^m) \frac{1}{\Delta Y} (f_y)_{j,k}(t_\kappa^m) \right] \quad (10)$$

to approximate the midpoint values  $s_{j,k}(t_\kappa^m + \frac{\Delta t_c}{2})$  since these values are bounded away from the jump discontinuities along the edges. In Eq. (10),

$$(f_x)_{j,k}(t_\kappa^m) = \Delta X \cdot \frac{\partial}{\partial x} f(s(x_j, y_k, t_\kappa^m)) + O(\Delta X)^2, \quad (f_y)_{j,k}(t_\kappa^m) = \Delta Y \cdot \frac{\partial}{\partial y} f(s(x_j, y_k, t_\kappa^m)) + O(\Delta Y)^2, \quad (11)$$

are the discrete fluxes in the  $x$  and  $y$  directions, respectively.

In our sequential scheme, when solving for the saturation in time, the total velocity  $\mathbf{v}$  is given by the solution of the velocity-pressure equation. Recall that the solution of Eq. (1) utilizes the lowest order Raviart-Thomas mixed finite element method. Thus, the computed total velocity  $\mathbf{v}$  is discontinuous at the vertices of the original non-staggered grid cells. This constitutes a difficulty for the staggered scheme (9), which requires the values of the total velocity  $\mathbf{v}$  at these vertices at every other time step. To skip this difficulty we employ the non-staggered version of the NT scheme.

To turn the staggered scheme (9) into a non-staggered scheme, we re-average reconstructed values of the underlying staggered scheme, thus recovering the cell averages of the

central scheme over the original non-staggered grid cells. First we reconstruct a piecewise bilinear interpolant at the time step  $t = t_\kappa^m + \Delta t_c$

$$\begin{aligned} P_{j+\frac{1}{2},k+\frac{1}{2}}(x, y, t) &= s_{j+\frac{1}{2},k+\frac{1}{2}}(t) + (x - x_{j+\frac{1}{2}}) \frac{1}{\Delta X} (s_x)_{j+\frac{1}{2},k+\frac{1}{2}}(t) \\ &+ (y - y_{k+\frac{1}{2}}) \frac{1}{\Delta Y} (s_y)_{j+\frac{1}{2},k+\frac{1}{2}}(t), \quad x_j \leq x \leq x_{j+1}, \quad y_k \leq y \leq y_{k+1}, \end{aligned} \quad (12)$$

as in (5), through the staggered cell averages given by (9), and re-averaged it over the original grid cells, giving the following non-staggered scheme also at  $t = t_\kappa^m + \Delta t_c$ :

$$\begin{aligned} s_{j,k}(t) &= \frac{1}{4} (s_{j-\frac{1}{2},k-\frac{1}{2}}(t) + s_{j-\frac{1}{2},k+\frac{1}{2}}(t) + s_{j+\frac{1}{2},k-\frac{1}{2}}(t) + s_{j+\frac{1}{2},k+\frac{1}{2}}(t)) \\ &+ \frac{1}{16} ((s_x)_{j-\frac{1}{2},k-\frac{1}{2}}(t) + (s_x)_{j-\frac{1}{2},k+\frac{1}{2}}(t) - (s_x)_{j+\frac{1}{2},k-\frac{1}{2}}(t) - (s_x)_{j+\frac{1}{2},k+\frac{1}{2}}(t)) \\ &+ \frac{1}{16} ((s_y)_{j-\frac{1}{2},k-\frac{1}{2}}(t) - (s_y)_{j-\frac{1}{2},k+\frac{1}{2}}(t) + (s_y)_{j+\frac{1}{2},k-\frac{1}{2}}(t) - (s_y)_{j+\frac{1}{2},k+\frac{1}{2}}(t)). \end{aligned} \quad (13)$$

**Remark:** The numerical derivatives (6) and (11) are required to produce a second order scheme for the approximation of (3) and to avoid oscillations, it is essential to reconstruct these discrete derivatives with built-in nonlinear limiters [Le Veque, 1990] and [Nessyahu, et al., 1990]. We refer to the reader to [Nessyahu, et al., 1990] (and the references therein) for the various options of the form of such discrete derivatives. We refer to [Abreu, et al., 2004a] for a carefully discussion for our choice of the form of the numerical derivatives.

**3.2. The Kurganov-Tadmor central scheme for two-phase flows.** In order to reduce the numerical diffusion of the NT scheme, Kurganov and Tadmor combined ideas from the construction of the NT scheme with the method of Rusanov, ([Rusanov, V., 1961]). The Rusanov method is also called the Local Lax-Friedrichs' method since it has the same form of the LxF method with the viscosity coefficient given by the local speed of wave propagation computed at each Riemann problem. These local speeds are used to average the non-smooth parts of the computed solution over smaller cells of variable size of order  $O(\Delta t)$  and are the only additional information required to modify the NT scheme. The lower numerical viscosity, of order  $O(\Delta X^3)$ , is independent of  $1/\Delta t$ . With this new feature, and letting  $\Delta t \downarrow 0$ , Kurganov and Tadmor obtained the first second order central scheme that admits a particularly simple semi-discrete formulation. This scheme also enjoys a non-oscillatory property guaranteed by a scalar maximum principle in two space dimensions (see [Kurganov, et al., 2000] for details).

First consider the model of hyperbolic conservation laws as described in section 3.1 by the equation (3) with cell averages defined in (4). So, to find approximate solution to (3), we follow the construction of the KT scheme in its fully discrete formulation in two space dimensions as explained in [Kurganov, et al., 2000]. Letting  $\Delta t \downarrow 0$ , we obtain a semi-discrete formulation written in conservative form as

$$\frac{d}{dt} s_{jk}(t) = - \frac{H_{j+1/2,k}^x(t) - H_{j-1/2,k}^x(t)}{\Delta X} - \frac{H_{j,k+1/2}^y(t) - H_{j,k-1/2}^y(t)}{\Delta Y}. \quad (14)$$

where

$$H_{j+1/2,k}^x(t) := \frac{1}{2} \left\{ v_{j+1/2,k}^x(t) [f(s_{j+1/2,k}^+(t)) + f(s_{j+1/2,k}^-(t))] \right\} \\ - \frac{a_{j+1/2,k}^x(t)}{2} [s_{j+1/2,k}^+(t) - s_{j+1/2,k}^-(t)],$$

$$H_{j,k+1/2}^y(t) := \frac{1}{2} \left\{ v_{j,k+1/2}^y(t) [f(s_{j,k+1/2}^+(t)) + f(s_{j,k+1/2}^-(t))] \right\} \\ - \frac{a_{j,k+1/2}^y(t)}{2} [s_{j,k+1/2}^+(t) - s_{j,k+1/2}^-(t)],$$

are the numerical fluxes in the  $x$  and  $y$  directions, respectively, and they can be viewed as a generalization of the one-dimensional numerical flux constructed in [Kurganov, et al., 2000]. The values  $s_{j+1/2,k}^\pm(t)$  and  $s_{j,k+1/2}^\pm(t)$  given by

$$s_{j+1/2,k}^\pm(t) = s_{j+1/2(\pm 1/2),k}(t) \mp \frac{\Delta X}{2} (s_x)_{j+1/2(\pm 1/2),k}(t), \\ s_{j,k+1/2}^\pm(t) = s_{j,k+1/2(\pm 1/2)}(t) \mp \frac{\Delta Y}{2} (s_y)_{j,k+1/2(\pm 1/2)}(t),$$

are obtained at each cell boundary intersecting the line segments  $y = y_k$  and  $x = x_j$ , respectively, with the reconstructed plane described in (5) and (6).

The local speeds of wave propagation in the  $x$  and  $y$  directions are estimated at the cell boundaries  $x_{j+1/2}$  e  $y_{k+1/2}$ , respectively, by the upper bounds

$$a_{j+1/2,k}^x(t) = \max\{|f'(s)| : s_{j+1/2,k}^- \leq s \leq s_{j+1/2,k}^+\}, \quad (15)$$

$$a_{j,k+1/2}^y(t) = \max\{|f'(s)| : s_{j,k+1/2}^- \leq s \leq s_{j,k+1/2}^+\}. \quad (16)$$

Here the velocity field  $\mathbf{v}$  (see Eq. (1)) used in the KT scheme is obtained directly from Raviart-Thomas space on the faces of the cells:

$${}^x v_{j+1/2,k}(t) = (v_r)_{jk}(t), \quad {}^x v_{j-1/2,k}(t) = (v_l)_{jk}(t), \quad (17)$$

$${}^y v_{j,k+1/2}(t) = (v_u)_{jk}(t), \quad {}^y v_{j,k-1/2}(t) = (v_d)_{jk}(t), \quad (18)$$

where  $v_r, v_l, v_u, v_d$  stand for the velocity on the “right”, “left”, “up” and “down” faces of the cells.

Suppose the solution is computed at some time level  $t = t_\kappa^m$  and it is approximated by a two-dimensional, non-oscillatory piecewise linear polynomial as given in (5) and (6). The non-oscillatory spatial derivatives in both,  $x$  and  $y$  directions are estimated using the MinMod Limiter with three points (see [Kurganov, et al., 2000, Nessyahu, et al., 1990]).

The time evolution of the semi-discrete equation (14) (ordinary differential equation) is carried out by the third order explicit embedded integration Runge-Kutta methods.

**Remark:** In the time-marching algorithm introduced in section 2 for the solution of the scalar hyperbolic conservation law (3) in semi-discrete formulation the saturation equation is approximated at times  $t_\kappa^m = t^m + \kappa \Delta t_c$  for  $t^m < t_\kappa^m \leq t^{m+1}$  to take into account the convective transport of water.

#### 4. TWO-DIMENSIONAL NUMERICAL EXPERIMENTS

We present and compare the results for numerical simulations of two-dimensional, two-phase flow associated with two distinct flooding problems using the KT and NT schemes. 1) Two-dimensional flow in a rectangular, heterogeneous reservoir (*slab geometry*) having  $256 \text{ m} \times 64 \text{ m}$  and, 2) Two-dimensional flow in a 5-spot pattern, homogeneous reservoir having  $64 \text{ m} \times 64 \text{ m}$ . In all simulations, the reservoir contains initially 79% of oil and 21% of water. Water is injected at a constant rate of 0.2 pore volumes every year.

The fractional volumetric flow, the total mobility, and the relative permeabilities are assumed to be:

$$f(s) = \frac{k_{rw}(s)/\mu_w}{\lambda(s)}, \quad \lambda(s) = \frac{k_{rw}(s)}{\mu_w} + \frac{k_{ro}(s)}{\mu_o},$$

and

$$k_{ro}(s) = (1 - (1 - s_{ro})^{-1}s)^2, \quad k_{rw}(s) = (1 - s_{rw})^{-2}(s - s_{rw})^2,$$

where  $s_{ro} = 0.15$  and  $s_{rw} = 0.2$  are the residual oil and water saturations, respectively. The viscosity of oil and water used in all simulations are  $\mu_o = 5.0 \text{ cP}$  and  $\mu_w = 0.05 \text{ cP}$ .

For the heterogeneous reservoir studies we consider a scalar absolute permeability field  $K(\mathbf{x})$  taken to be log-normal (a fractal field, see [Glimm, J., et al., (1993)] and [Furtado, et al., 2003] for more details) with moderately large heterogeneity strength. The spatially variable permeability field is defined on  $256 \times 64$  grid with the coefficient of variation  $C_v$  (mean/(standard deviation)): 0.5.

The boundary conditions and injection and production specifications for two-phase flow equations (1)-(2) are as follows. For the horizontal slab geometry, injection is made uniformly along the left edge of the reservoir and the (total) production rate is taken to be uniform along the right edge; no flow is allowed along the edges appearing at the top and bottom of the reservoir in the graphics.

In the case of a five-spot flood, injection takes place at one corner and production at the diametrically opposite corner; no flow is allowed across the entirety of the boundary.

We now discuss the simulations in the slab geometry. Figure 2 refers to a comparative study for the NT and KT schemes, showing the water saturation surface plots after 350 days of simulation. The results using the NT scheme were computed with grids having  $256 \times 64$ ,  $512 \times 128$  and  $1024 \times 256$  cells (the first three from top to bottom). One simulation used the KT scheme on a  $256 \times 64$  computational grid (the last one, from top to bottom). Note that the KT scheme gives a more accurate solution than the solutions computed by the NT scheme. This numerical result seems to be in agreement with the smaller amount of numerical viscosity, independent of  $1/\Delta t$  [Kurganov, et al., 2000]. The smaller amount of dissipation enables efficient integration of convection equations, where the accumulated error is independent of a small time step dictated by the CFL limitation [Kurganov, et al., 2000].

We discuss next the set of simulations performed in a 5-spot pattern, homogeneous reservoir. Figure 3 shows the saturation level curves after 260 days of simulation obtained with both NT and KT schemes, for two levels of spatial discretization. The plots on the left column are the results obtained with the NT scheme and the ones on the right were computed with the KT scheme. The grids are finer from top to bottom and have  $64 \times 64$  and  $128 \times 128$  cells, respectively. It is clear that the KT scheme is producing incorrect



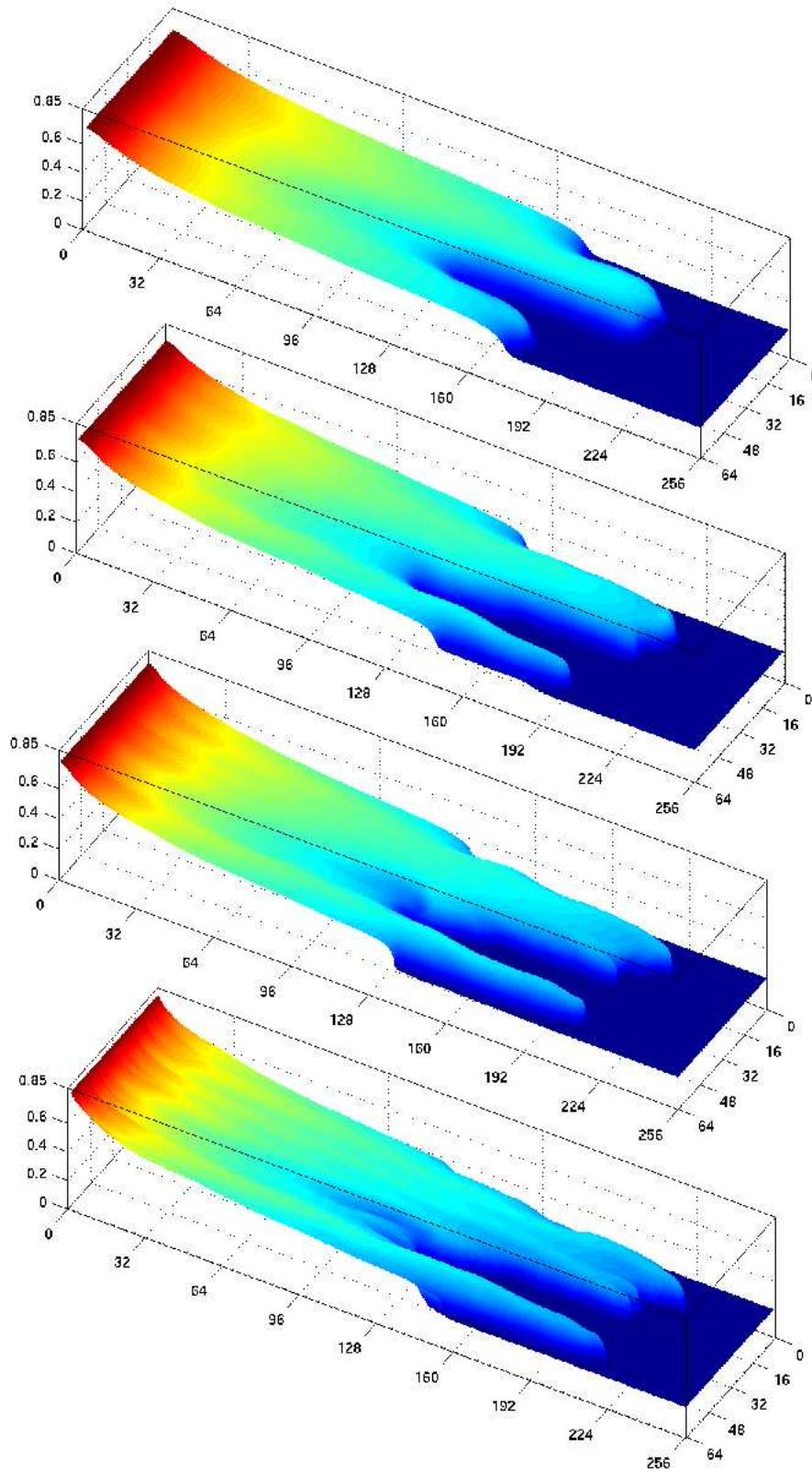


FIGURE 2. Water saturation surface plots for two-phase flow in a two-dimensional rectangular heterogeneous reservoir having  $256 \text{ m} \times 64 \text{ m}$ . From top to bottom, the NT scheme was used for the first three plots and the KT scheme was used for the one at the bottom.

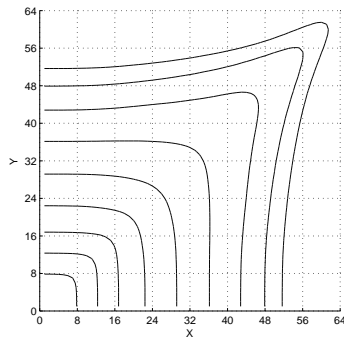
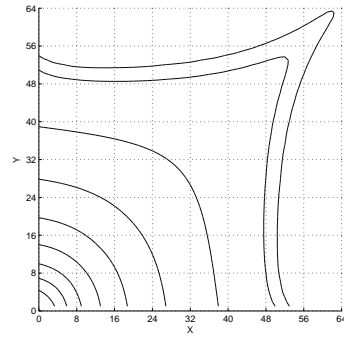
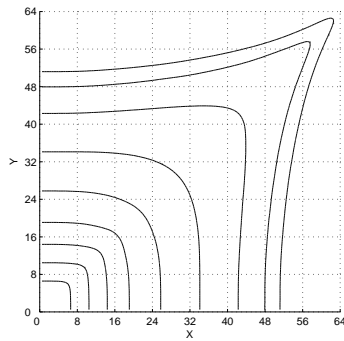
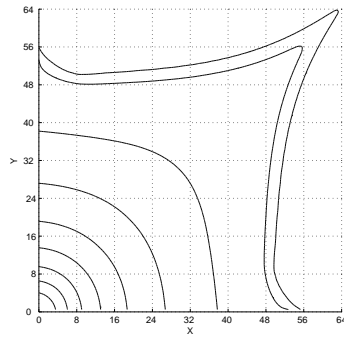
(a) NT:  $64 \times 64$  grid(b) KT:  $64 \times 64$  grid(c) NT:  $128 \times 128$  grid(d) KT:  $128 \times 128$  grid

FIGURE 3. Water saturation level curves for two-phase flow in a 5-spot geometry. The NT (KT) scheme was used in (a) and (c) ((b) and (d)).

boundary behavior; moreover, as the computational grid is refined this problem seems to be emphasized. Although considerable less diffusive, the KT schemes produces incorrect results for this two-dimensional problem.

The KT scheme uses numerical fluxes in the  $x$  and  $y$  directions which can be viewed as generalizations of one-dimensional numerical fluxes. We conjecture that this type of approximation for the fluxes leads to the incorrect boundary behavior discussed above. If this conjecture is correct one might be able to improve the boundary behavior by deriving a new multidimensional version of the KT scheme, starting from a multidimensional version of the NT scheme. The authors are currently developing such scheme.

## REFERENCES

- Abreu, et al., 2004a. Abreu, E., J. Douglas, Jr., F. Furtado, D., Marchesin, and F., Pereira. (2004) *Three-Phase Immiscible Displacement in Heterogeneous Petroleum Reservoirs*. To appear in the Journal of Applied Numerical Mathematics.

- Abreu, et al., 2004b. Abreu, E., F. Furtado, D., Marchesin, and F., Pereira (2004), *Transitional Waves in Three-Phase Flows in Heterogeneous Formations*. Computational Methods for Water Resources, edited by C. T. Miller, M. W. Farthing, W. G. Gray and G. F. Pinder, Series: Developments in Water Science, **I**, 609-620, Chapel Hill, NC, USA.
- Abreu, et al., 2004c. Abreu, E., F. Furtado, D., Marchesin, and F., Pereira, (to appear) *Three-Phase Flow in Petroleum Reservoirs*. Proceedings of the Conference on Analysis, Modeling and Computation of PDEs and Multiphase Flow, in Celebration of James Glimm's 70th Birthday, SUNY at Stony Brook, New York.
- Abreu, et al., 2004d. Abreu, E., F. Furtado, and F., Pereira (2004), *On the Numerical Simulation of Three-Phase Reservoir Transport Problems*. Transport Theory and Statistical Physics, **33** (5-7), 503-526.
- Chavent, et al., 1986. Chavent, G. and Jaffre, J. (1986), *Mathematical Methods and Finite Elements for Reservoir Simulation*, Studies in Mathematics and its Applications, 17 North-Holland, Amsterdam, 390 pp.
- Douglas, J., Jr., et al., 1997. Douglas, J. Jr., F. Furtado, and F. Pereira (1997), *On the numerical simulation of waterflooding of heterogeneous petroleum reservoirs*. Computational Geosciences 1(2), 155-190.
- Furtado, et al., 2003. Furtado F, Pereira F. (2003), *Crossover from nonlinearity controlled to heterogeneity controlled mixing in two-phase porous media flows*, Computational Geosciences, **7**, 115-135.
- Glimm, J., et al., (1993). Glimm, J., Lindquist, B., Pereira, F., and Zhang, Q. (1993), *A theory of macrodispersion for the scale up problem*. Transport in Porous Media, **13**, 97-122.
- Nessyahu, et al., 1990. Nessyahu, N., and Tadmor, E. (1990), *Non-oscillatory central differencing for hyperbolic conservation laws*, Journal of Computational Physics, **87**, No. 2, 408-463.
- Harten, A., et al., 1987. Harten, A. and Osher, S. (1987), *Uniformly High Order Accurate Non-Oscillatory Scheme I*, SINUM **24**, 279-309.
- Kupferman, R., et al., 1997. Kupferman, R. and Tadmor, E. (1997), *A fast high resolution second order central scheme for incompressible flows*, Proc. Natl. Acad. Sci. USA, May 13, 94 (10), 4848-4852.
- Kurganov, et al., 2000. Kurganov, A. and Tadmor, E. (2000), *New high resolution central schemes for nonlinear conservation laws and convection-diffusion equations*. Journal of Computational Physics, **160**, 214-282.
- Le Veque, 1990. Le Veque, J. R. (1990), *Numerical methods for conservation laws*. Lectures in mathematics, Basel, Boston, Berlin.
- D. W. Peaceman, 1977. D. W. Peaceman (1977), *Fundamentals of Numerical Reservoir Simulation*, Elsevier, New York.
- Raviart P-A., et al., 1977. Raviart P-A., and Thomas, J. M. (1977), *A mixed finite element method for second order elliptic problems*, 1977, in "Mathematical Aspects of the Finite Element Method", Lecture Notes in Mathematics, edited by I. Galligani, and E. Magenes, **606**, 292-315, Springer-Verlag, Berlin, New Yorkes.
- Rusanov, V., 1961. Rusanov, V. V. (1961), *Calculation of interaction of non-steady shock waves with obstacles*, J. Comp. Math. Phys. USSR, **1**, 267-279.